NEW INVESTIGATIONS OF COLOR VARIATION ON EROS. Lauren M. Jozwiak[1] and David T. Blewett[1], [1]Planetary Exploration Group, Johns Hopkins University Applied Physics Laboratory, Laurel, MD, USA (lauren.jozwiak@jhuapl.edu).

Introduction: The Near Earth Asteroid Rendezvous (NEAR) – Shoemaker mission performed an orbital investigation of the near-Earth asteroid 433 Eros from 2000-2001 [1] returning the first orbital images of an asteroid. While Eros harbors intriguing surface features, such as ponds [e.g. 2, 3] and boulders [2], it displayed seemingly few color variations. The perception of color blandness was reinforced by the limited spectral variation found in data from the NEAR Near-Infrared Spectrometer (NIS), which shows only very subtle variations in the center or shape of the 1-μm mafic mineral absorption band [e.g. 4]. However, the spatial resolution of the NIS footprints are quite large compared with the pixel dimensions of images obtained by the Multi-Spectral Imager (MSI), and thus the true question of color variation on Eros is underexplored.

Unfortunately, because of a failed orbital insertion maneuver in 1998, tens of kilograms of hydrazine burn products were expended by spacecraft thrusters, and caused condensation on MSI optical surfaces [5, 6]; images from filters 2 and 7 could not be recovered with sufficient quality for spectral analysis [7], and the remaining filters required the application of significant deblurring procedures [7, 8]. Although deblurring was able to restore the data from the remaining 5 filters (1, 3, 4, 5, and 6) a majority of analyses only utilized two or three filters (primarily filters 1, 3, and 4, 550 nm, 760 nm, and 950 nm, respectively) [9, 10]. Therefore, there remains a set of unexplored color data in the unexploited filters 5 and 6 (900 and 1000 nm).

Here we describe our efforts to establish a procedure for investigating the full suite of Eros color variations, including our process for photometrically normalizing and coregistering the images, identifying image sets for features of interest, and initial products.

Photometric Correction and Coregistration: R. Gaskell and colleagues have produced a high-resolution Eros shape model [11] using the technique of stereophotoclinometry [12]. We registered nearly all the MSI images of Eros to the Gaskell shape model, and produced a set of updated backplanes for geometric and geophysical parameters including incidence, emergence, and phase angles [13]. These backplanes allowed us to perform photometric normalization using the model of [14], adjusting the images to standard illumination and viewing conditions (incidence = phase = 30°, emergence = 0°), with improved fidelity compared to the older, lower-resolution shape model of Thomas [15] (Fig. 1).

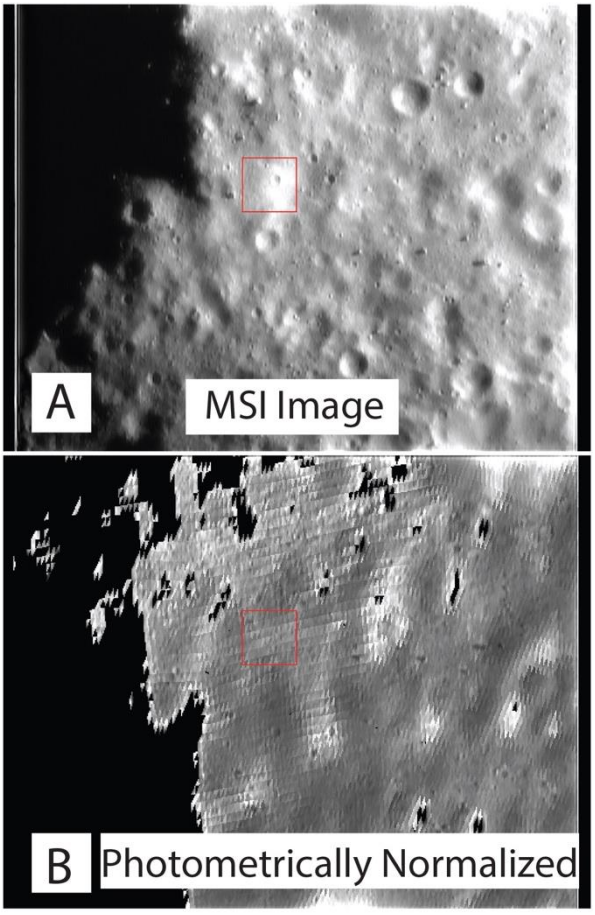

Figure 1: Comparison of MSI image M0132590164F4 before (A) and after (B) photometric normalization.

Small Body Mapping Tool: The Small Body Mapping Tool (SBMT) [16] is an interactive tool for visualizing spacecraft data on small bodies. The SBMT is publically available at http://sbmt.jhuapl.edu/ . Among the capabilities of the tool is the ability to ingest custom images (in this case the photometrically normalized MSI images), project them onto the shape model, and to output these images as a cube file comprised of co-registered images (Fig. 2). Thus we are able to identify overlapping sets of images, and produce files that are suitable for spectral and color analysis in programs such as ENVI.

Color Analysis Objectives: With a process in-place for analyzing color variations on Eros, we now outline the features that have previously been suggested to have minimal color variation, and the features we will be investigating with this new process.

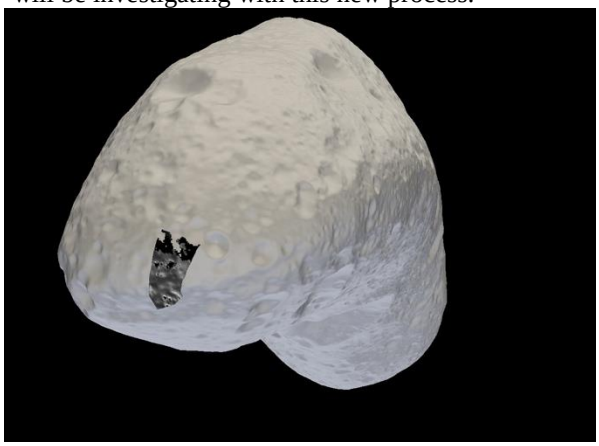

Figure 2: Perspective view of an SBMT generated image cube. The cube was produced from 5 images, and the cube extent is defined by the overlapping regions shared by all 5 input images.

Initial analysis of MSI data identified four distinct color units: bright streaks, dark soils, ponded materials, and average regolith [e.g. 2, 3, 9, 10]. Despite the color and albedo variations associated with these terrains, they are thought to be associated with regolith transport and sorting processes, and are not indicative of compositional variations [e.g. 4, 17, 18]. Riner et al. (2008) [10] used ratio plots of bands 1, 3, and 4 to separate the four color units, but noted that photometric normalization of the images would improve these efforts. The authors observed that bright streaks, dark soils, and average regolith fall on a mixing line consistent with the effects of space weathering; however, ponded materials did not fall on this trend line [10]. This observation is also consistent with the early observation that ponded materials were "bluer" than surrounding regions [3].

Using image sets that have undergone photometric normalization, we will repeat the analysis of [10] to further examine the degree of unit separation, and to investigate whether the previously observed trends are maintained, or whether normalization separates color units from the previously observed trendlines. We will also examine multiple ponded deposits to determine if these units are consistently bluer than surrounding materials. A new listing of Eros geologic features, including ponds, that gives improved location information has recently been produced [19].

Conclusions: Using a combination of coregistration and photometric normalization, and leveraging new capabilities in the Small Body Mapping Tool, we have developed a processing pathway for re-investigating color variations on Eros. Our process will allow us to more fully investigate both previously observed color trends, and also to explore the potential for previously unrecognized color variations using the underutilized MSI filters 5 and 6.

References: [1] Cheng, A. F., et al. (1997) *JGR 102*, 23695-23708. [2] Veverka, J. et al. (2001) *Science 292*, 484-488. [Robinson, M. S., et al. (2002) *M&PS 37*, 1095-1105. [4] Bell, J. F., et al. (2002) *Icarus 155*, 119-144. [5] Yeomans, D. K., et al. (1999) *Science 285*, 560-561. [6] Veverka, J., et al. (1999) *Science 285*, 562-564. [7] Murchie, S., et al. (2002) *Icarus 155*, 229-243. [8] Li, H., et al. (2002) *Icarus 155*, 244-252. [9] Murchie, S., et al. (2002) *Icarus 155*, 145-168. [10] Riner, M. A., et al. (2008) *Icarus 198*, 67-76. [11] Gaskell, R.W. (2008), NEAR-A-MSI-5-EROSSHAPE-V1.0, NASA PDS. [12] Gaskell, R.W. et al. (2008), *M&PS 43*, 1049–1061. [13] Blewett, D.T. et al., (2017) urn:nasa:pds:nearmsi.shapebackplane. NASA PDS. [14] Clark, B.E. et al. (2002), *Icarus 155*, 189–204. [15] Thomas, P.C., et al. (2002), *Icarus 155*, 18–37. [16] Kahn, E. M., et al. (2011) *LPSC 42*, Abstract #1608. [17] McCoy, T. J., et al. (2001) *M&PS 36*, 1661-1672. [18] McFadden, L. A., et al. (2001) *M&PS 36*, 1711-1726. [19] Roberts, J.H. et al. (2019) *LPSC 50*, abstract #1494.